Epilepsy Research (2010) **91**, 133—142

journal homepage: www.elsevier.com/locate/epilepsyres

Imaging foci of epileptic discharges from simultaneous EEG and fMRI using the canonical HRF

Cheng Luo[a], Zhiping Yao[b], Qifu Li[b,c], Xu Lei[a], Dong Zhou[b], Yun Qin[a], Yang Xia[a], Yongxiu Lai[a], Qiyong Gong[d,*], Dezhong Yao[a,]**

[a] *Key Laboratory for NeuroInformation of Ministry of Education, School of Life Science and Technology, University of Electronic Science and Technology of China, Chengdu, China*
[b] *Department of Neurology, West China Hospital, Sichuan University, Chengdu, China*
[c] *Department of Neurology, The Affiliated Hospital of Hainan Medical College, Haikou, China*
[d] *Huaxi MR Research Center, Department of Radiology, West China Hospital, Sichuan University, Chengdu, China*

Received 26 February 2010; received in revised form 29 June 2010; accepted 4 July 2010
Available online 31 July 2010

KEYWORDS
IEDs classification;
EEG—fMRI;
Epilepsy;
GLM;
Localization

Summary
Purpose: Simultaneous electroencephalography and functional magnetic resonance imaging (EEG—fMRI) is considered as a powerful and non-invasive method that allows definition of the irritative zone. However, the complex interictal epileptic discharge (IED) may be present in some patients, and sometimes no active foci can be localized using General Linear Model (GLM) which is a widely adopted tool in EEG—fMRI study. The purpose of this study is to develop a new scheme to improve the detectability and localize the canonical HRF localizable foci.
Method: Various IEDs are classified using a combination of an independent component analysis (ICA) and a temporal correlation analysis between the independent components and the raw EEG channel; and the classified IEDs are then separately used for foci localization. This scheme is tested by ten patients with variable IEDs, including two patients whose activity could not be identified by common method.
Result: Applying this scheme to the two patients, some foci consistent with electroclinical data were localized. When it was applied to the remaining eight patients with positive results using common method, 2—4 types of IEDs were classified, and the activity could be identified from at least one type of IED. The results were similar to that received from common method.
Conclusion: These results indicate that the proposed scheme could enhance the imaging of the localizable foci by isolating its IEDs. This scheme is potentially a useful tool for epilepsy clinic.

* Corresponding author.
** Corresponding author. Tel.: +86 28 83201018; fax: +86 28 83208238.
E-mail addresses: dyao@uestc.edu.cn (D. Yao), qygong05@126.com (Q. Gong).

0920-1211/$ — see front matter © 2010 Elsevier B.V. All rights reserved.
doi:10.1016/j.eplepsyres.2010.07.003

Introduction

Simultaneous electroencephalogram (EEG) and functional magnetic resonance imaging (fMRI) has emerged as a useful and non-invasive technique for investigating interictal epileptic cerebral activity. The combination of two techniques provides considerable information to determine the irritative or epileptogenic zone. Since the introduction of this technology by Ives et al. (1993), has been developed and widely used in studies of epileptic patients with various forms of epilepsy seizure and among patients in all age groups (Kobayashi et al., 2006; Laufs et al., 2007; Gotman et al., 2005; Jacobs et al., 2007; Li et al., 2009; Luo et al., in press). Until now, both the data-driven method and model-driven method have been applied to mine EEG—fMRI data to determine BOLD changes responded to epileptic discharges (Gotman et al., 2006).The GLM framework (Friston et al., 1995) is a model-driven analysis method applied extensively in current fMRI practice (Gotman et al., 2006). The GLM model has also been heavily applied in the study of focal or general epilepsy with EEG—fMRI, resulting in valuable findings (Jacobs et al., 2007; Gotman et al., 2006; Laufs et al., 2008). In the investigation of epilepsy by EEG—fMRI, only approximately 60—80% of the cases have reported statistically significant BOLD changes in particular areas (Salek-Haddadi et al., 2006; Lu et al., 2006). In focal epilepsy, the sensitivity is even lower (Lemieux et al., 2008), while the reason is not clear. Based on our knowledge to date, the reasons for the limitations in sensitivity may include the following: (1) few interictal epileptic discharges (IEDs) decreasing the likelihood of detecting BOLD change (Salek-Haddadi et al., 2006). During the acquisition of fMRI data, it is not possible to predict when the epileptic discharges will occur, so the acquisition may meet no or few discharges. (2) Deep epileptic discharge in the brain may not be found in the scalp EEG. Due to the smearing effect of the volume conductor head, the scalp EEG may miss the discharge activity in the deep brain (Rodionov et al., 2007). (3) Using an unsuitable hemodynamic response function (HRF) in the GLM framework. The shape and latency of the hemodynamic response of IEDs are variable (Bénar et al., 2002; Lemieux et al., 2008; Lu et al., 2006), and in order to improve sensitivity, multiple HRFs, patient-specific HRFs, and different HRF peak latency have been tested in the GLM framework (Lu et al., 2006). In current practice, the canonical HRFs in SPM have been widely used in EEG—fMRI studies, and the reason may be that the nature of the hemodynamic response of an IED has not been fully described in a real data set.

In some epileptic disorders, different types of epileptic discharges may occur in a patient. These discharges arise from different brain regions or affect different brain regions, and the BOLD change caused by these discharges may have different shapes and delay times. Apparently, if the spikes can be properly classified, and the corresponding HRF can be adopted separately, the sensitivity of EEG—fMRI would be improved (Liston et al., 2006). However, the IED specific HRF is not easy to be determined. In this work, we focus on the patients with complex epileptic discharge, complex morphology in scalp EEG, and attempt to image the canonical HRF localizable foci by IEDs classification in EEG—fMRI studies. Because independent component analysis (ICA) has been adopted as a powerful tool for separating spikes of different origins (Urrestarazu et al., 2006), ICA is used to decompose the whole EEG data. A new scheme is introduced in this work. It includes that IEDs are classified using a combination of an ICA and a temporal correlation analysis between independent components and the raw EEG channel, and then each type of the isolated discharges is imaged using GLM. This scheme is applied to 10 sets of real EEG—fMRI data among which no activity is identified in two patients by the common method.

Methods

Scheme procedure

The algorithm procedure to analyze EEG—fMRI data was shown in Fig. 1.

Step 1: IEDs identification and raw EEG segmentation

IEDs were identified and marked by a clinically experienced neurophysiologist. The concatenation IED was considered as an IED in next analysis. For each IED, a time window which was a period from IED initiation to termination was marked. If the period of IED was less than 1 s, the time window was extended to 1 s for the subsequent procedure. So the time window was usually no shorter than 1 s. Meanwhile, a raw EEG segment in one channel that could predominantly represent this IED was chosen for the following correlation analysis.

Step 2: ICA of the raw EEG

The entire multichannel raw EEG data was decomposed by ICA with FastICA software (Hyvärinen, 1999), in which the number of independent components (ICs) was set at the accumulated rate of eigenvalues exceeding 99% after PCA dimension reduction. Both artifacts and EEGs generated by neural sources could be isolated. Then distinct artifact-related ICs were identified visually and discarded from further consideration. Epileptic discharges with different spatial distributions or temporal dynamic processes were considered as different epileptic events and they were usually decomposed into different ICs. One type of IED usually existed at one IC because ICs were characterized by their statistic properties (Comon, 1994). According to the onset and time window of each IED which were marked by expert, an IC matrix corresponding with an IED was created ($N \times T$, where N was the number of remaining ICs and T was the sample number of IED time window) (Fig. 1, Step 3).

Step 3: A scheme for IED classification

For each IED, temporal correlation coefficient (CC) was calculated respectively between N time courses in IC matrix and a representative channel of raw EEG segment marked by expert (Fig. 1, Steps 1—3). Here we adopted two procedures to classify the identified IEDs: (1) The best corresponding IC with maximum CC was obtained for each IED. (2) IEDs that had the same best corresponding IC were merged into one category (Fig. 1, IED1 and IED3), and the epileptic activity events in this IC (Fig. 1, IC1) were considered as the epileptic activity trains. So all IEDs were classified and used in subsequent analysis.

Step 4: fMRI data analysis

GLM was applied to image foci of each identified IED type. The SPM2 software package was used to analyze fMRI data (statistical parametric mapping http://www.fil.ion.ucl.ac.uk/spm). Preprocessing of fMRI data included the slice time correction, 3D motion detection and correction, spatial normalization to the MNI template supplied by SPM and spatial smoothing using an isotropic Gaussian kernel

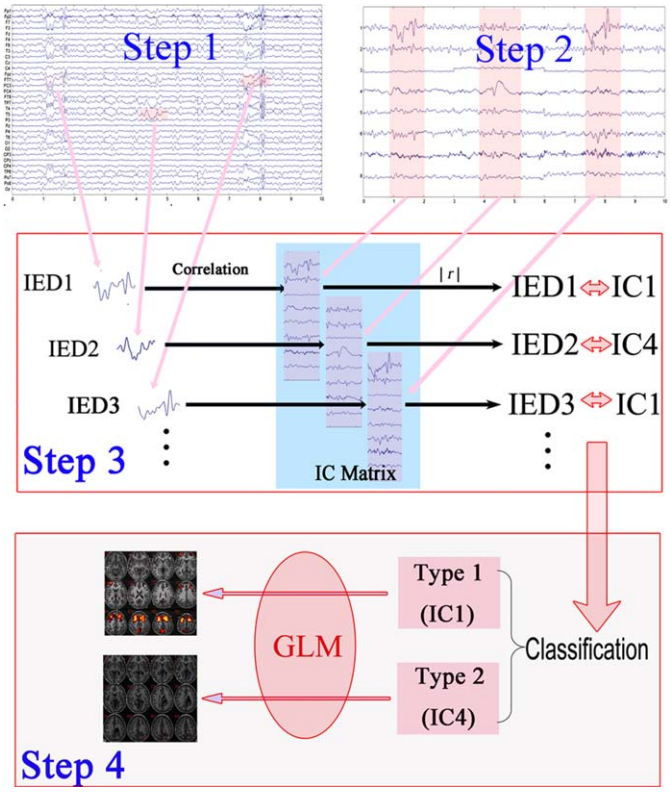

Figure 1 Schematic representation of data analysis. The raw EEG data was processed by an expert in Step 1. ICA was used in whole raw EEG in Step 2. Temporal correlation was calculated between a channel of raw EEG and each independent component with the same time windows in Step 3. Each IED was classified based on the different independent component which had the maximum correlation coefficient with a channel of raw EEG, such as the IED1 and IED3 as one type and the IED2 as the other type. In Step 4, the classified IED was used to model in SPM software package.

(6 mm full width at half maximum). Then, the canonical HRF in the SPM software package was convolved with each classified IEDs time pulse function, and the result was treated as an interested regressor in the SPM design matrices. Six parameters for the spatial realignment were included to model the linear and non-linear effects of meaningless head motion. Design matrices and data were high-pass filtered at 128 s cutoff. In order to estimate the intrinsic autocorrelation of the data, an autoregression (AR (1)) model was adopted

Table 1 Clinical details of patients.

Patient no.	Gender	Age	Onset (years)	Seizure type	Anatomy abnormality	Medication
1	M	13	2	CPS	Grey matter heterotopia in left temporal and occipital lobe, arachnoid cyst in left thalamus	TPM
2	M	10	1	CPS; SGTCS	Enlarged cisterna magna	VPA
3	M	13	2	CPS	Negative	TPM; CBZ
4	M	12	2	CPS; SGTCS	Negative	VPA; CBZ
5	M	11	1	SPS	Negative	None
6	M	19	16	CPS SGTCS	Grey matter heterotopia in left temporoparietal	CBZ; PB
7	F	12	1	CPS; SGTCS	Encephalomalacia in right frontal after injure	TCM
8	F	22	11	CPS; SGTCS	Negative	PHT; LTG;
9	F	21	2	SPS	Right hippocampus atrophy	CBZ; PB; TPM
10	M	18	6	CPS; SGTCS	Negative	CBZ; PB

Abbreviations: CPS: complex partial seizure; SGTCS: secondary generalized tonic–clonic seizure; SPS: simple pretrial seizure; CBZ: carbamazepine; LTG: lamotrigine; PB: phenobarbitone; PHT: phenytoin; TCM: traditional Chinese medicine; TPM: topiramate; VPA: sodium valproate

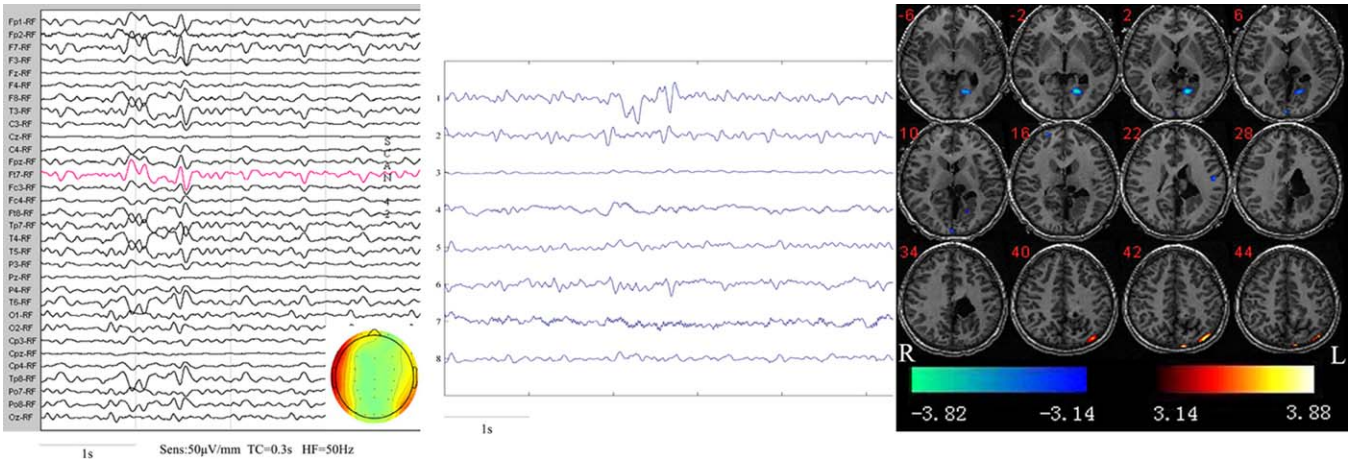

Figure 2 Patient 1 Type 1A IEDs. Type 1A comprised 12.5% of total IEDs in patient 1. Left: epileptic discharges recorded on the scalp in MR scanner, which was located at Ft7 F7 T3 Tp7 F8 T4. The topography of energy distribution during discharge was displayed. The channel with the red trace showed the clinically typical IEDs, as selected by the expert. Middle: IC segments from the same time window as on the left. IC1 was selected to represent Type 1A. Right: fMRI finding related to the corresponding Type 1A IEDs. Activation was observed in the periheterotopia, and deactivation was found in the lesioned and remote areas.

(Friston et al., 2000). The specially activated areas were calculated using statistical *t*-tests of each voxel. The significance level was set at $p < 0.05$ corrected with false discovery rate (FDR) (Christopher et al., 2002).

Patients

In total, 57 patients with epilepsy were recruited from the epilepsy clinics of the West China Hospital for Neurology, Sichuan University for an EEG—fMRI study from January 2006 to August 2008. All patients underwent 24-h video EEG. Diagnosis was established according to the diagnostic scheme published by the International League Against Epilepsy in 2001 (Engel, 2001). Informed consent for study participation was obtained from each patient. Data from a particular patient was used if the following two criteria were met: (1) more than ten IEDs were acquired; (2) no significant activity was found by SPM with whole IEDs and the canonical HRF. Based on these criteria, EEG—fMRI data of 2 patients were obtained from 57

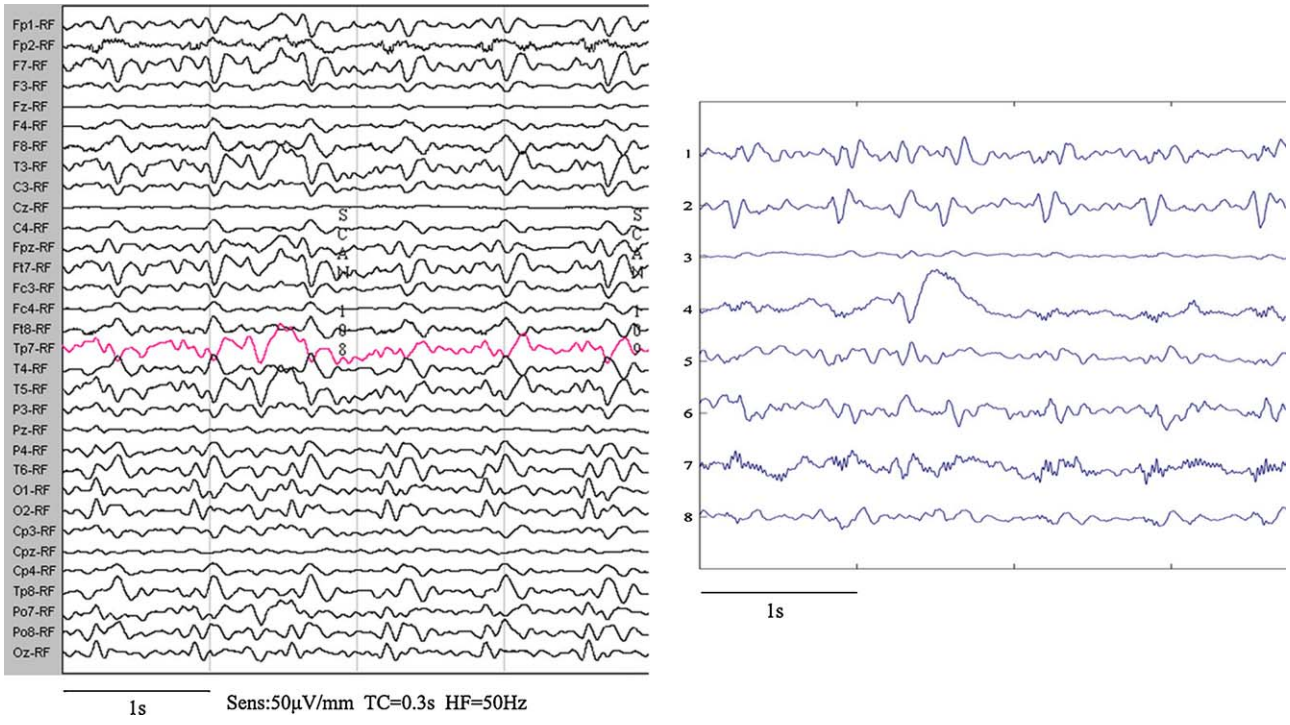

Figure 3 Patient 1 Type 1B IEDs. Type 1B comprised 87.5% of total IEDs in patient 1. Left: epileptic discharges recorded on the scalp in MR scanner, which was located at Fp7 T3 T5 Ft7 F7. The channel with the red trace showed the clinically typical IEDs, as identified by the expert. Right: IC segment from the same time window as on the left. IC4 was selected to represent Type 1B. No activity related to these IEDs was found.

Table 2 Summary of IEDs classification and fMRI activity for 10 patients.

Patient's category of IED	The number of IEDs	Percent of IEDs	Scalp EEG location of IEDs	fMRI activity	
				Activation	Deactivation
1_all	24			None	None
1A	3	12.5%	L(preF,F,T)	L(O,P)	L(O,F); R(F,limbic lobe)
1B	21	87.5%	L(F,T)	None	None
2_all	19			None	None
2A	4	21.1%	widespread	B(F,T,P,O,Th)	None
2B	1	5.2%	L(preF,T)	B(F)	L(T)
2C	11	57.9%	L(C,P,O)	None	None
2D	3	15.8%	B(F)	None	None
3_all	19			B(F,P);L(O,Cb)	B(T,F)
3A	11	58%	B(F);C	B(F,P);L(O,Cb)	B(T, F)
3B	8	42%	R(O,P)	None	None
4_all	16			B(F,P,Th);L(T)	B(T,F); R(P,O)
4A	12	75%	L(P,C)	B(F,Th); L(T)	B(T,F); R(P,O)
4B	4	25%	B(T,P)	None	None
5_all	18			R(Gp,T,F)	Cb; Cg;
5A	9	50%	R(T,P)	R(Gp,T);L(F)	Cb; Cg; R(T)
5B	5	28%	L(F,T);B(C)	B(F,P)	None
5C	4	22%	B(F,C)	None	None
6_all	43			B(F,T,P,Th)	B(P,T,F,Cn); Cb
6A	27	63%	L(P,T)	B(F,T,P,Th)	B(P,T,F,Cn); Cb
6B	8	19%	B(F)	R(F,P)	None
6C	3	7%	B(F,T,P,O)	B(F,Th)	B(P,T,Cn,Cg); Cb
6D	5	11%	L(O,R,T)	None	None
7_all	16			B(T); R(Hg)	B(F,Th,Gp,Cg); R(P)
7A	9	56%	B(F)	B(Hg); R(T)	R(P,Cg,Cn)
7B	4	25%	R(F,T)	R(T,Th);L(P,F)	None
7C	3	19%	R(C,T,P)	B(T,P,O)	B(F,T); Cb
8_all	14			B(F,P,Th); L(T)	B(T,F); R(P,O)
8A	10	71%	R(O,P)	R(O,P);L(F,Th)	B(F); some white matter
8B	4	29%	B(T,P)	B(F,P);L(O,T)	B(F,P,Cn)
9_all	12			B(T)	None
9A	10	83%	R(T,O)	B(T);R(Hg)	None
9B	2	17%	B(T,F)	R(O)	B(O)
10_all	22			B(T,P)	R(O,Cg); Cb;
10A	14	64%	R(T)	B(T,P); R(Th)	B(F,P); R(Cg,Cn)
10B	5	23%	B(T)	R(T,P)	B(F,P)
10C	3	13%	L(T,P)	None	None

Abbreviations: L: left lateral; R: right lateral; B: bilateral; T: temporal; F: frontal; C: central; P: parietal; O: occipital; Cb: cerebellum; Hg: hippocampus gyrus; Cg: cingulated gyrus; Th: thalamus; Cn: caudate nucleus; Gp: globus pallidus.

patients. Besides, to see the performance of the proposed scheme which was applied to other cases, in which some active regions could be identified from the fMRI data by the common method, eight patients with complex epileptic discharges were selected. Clinic details and demographic characteristics of the 10 patients selected were presented in Table 1.

Data acquisition and IED identification

FMRI data were acquired using gradient-echo echo-planar imaging (EPI) sequences in a 3T MRI scanner (EXCITE, GE Milwaukee, USA) with an eight-channel phased array head coil. The imaging parameters were as follows: thickness = 5 mm (no gap), TR = 2000 ms, TE = 30 ms, FOV = 24 cm × 24 cm, flip angle = 90°, and matrix = 64 × 64. Two hundred and five volumes (30 slices per volume) were acquired during the 410 s fMRI run. In order to ensure steady-state of longitudinal magnetization, the first five volumes were discarded. Anatomical T1-weighted images were acquired using a three-dimensional (3D) spoiled gradient recalled (SPGR) sequence, resulting in 156 axial slices (thickness = 1 mm (no gap), TR = 8.5 ms, TE = 3.4 ms, FOV = 24 cm × 24 cm, flip angle = 12°, and matrix = 512 × 512). During fMRI acquisition, EEG data were recorded continuously (EBNeuro, Florence, Italy). The MR artifact was filtered out (Garreffa et al., 2003), and the EEG was analyzed by an experienced neurophysiologist who identified IEDs and marked the times of the IED on a typical raw EEG channel.

Results

Using our proposed scheme, more than one type of IEDs were identified for every patient. The number of IED, their location, their categories and responding fMRI activity of 10 patients were illustrated in Table 2.

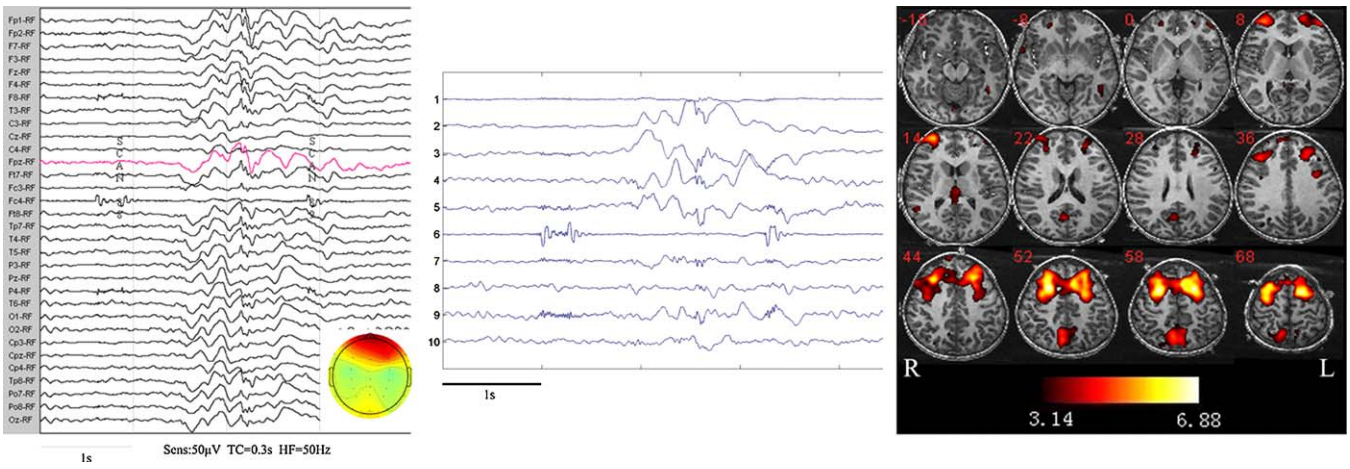

Figure 4 Type 2A IEDs in patient 2. Left: generalized epileptic discharges recorded from the scalp in MR scanner. The high amplitude slow wave activity was distributed generally in scalp and predominant at bilateral frontal regions. The topography of energy distribution during discharge was displayed. The channel with the red trace showed the clinically typical IEDs, as selected by the expert. Middle: IC segments from the same time window as on the left. IC2 was selected to represent Type 2A. Right: fMRI results related to these IEDs. The activations were observed in the bilateral cortices and thalamus, particularly in the bilateral frontal and parietal lobes. No deactivation was found.

Twenty-four and nineteen IEDs were identified for patients 1 and 2 by the expert, respectively. For patient 1, eight ICs were obtained by ICA, and two categories were identified by correlation analysis, including 3 IEDs of Type 1A by IC1 (Fig. 2) and 21 IEDs of Type 1B by IC4 (Fig. 3). For patient 2, ten ICs and four categories were classified. Using the proposed scheme, 4 types of IEDs were classified: Type 2A by IC2 (4 IEDs observed; Fig. 4), Type 2B by IC8 (1 IED observed; Fig. 5), Type 2C by IC4 (11 IEDs observed; Fig. 6), and Type 2D by IC3 (3 IEDs observed; Fig. 6).

For patient 1, significant BOLD activity was revealed in the lesioned area of the brain associated with Type 1A IEDs (12.5%) (Fig. 3), while no significant activity was found for Type 1B IEDs (87.5%). For patient 2, BOLD activities associated with Type 2A (21.1%) and 2B (5.2%) were found (Figs. 4 and 5), whereas no significant activity was found for Type 2C (57.9%) and 2D (15.8%) IEDs. In addition, no significant activity was found when Type 2B, 2C and 2D were classified as one type in a primary visual classification. For the two patients, the activity was absent in the IED category with the largest ratio (Type 1B and Type 2C)

In the remaining eight patients, some active regions were found by SPM with whole IEDs and the canonical HRF (common method). Two categories of IEDs were found in four patients, three categories in three patients and four categories in a patient. Using the newly proposed scheme, we observed that the activity could be obtained from at least one type of IED for every subject, and the map resulted from a type usually similar to that without classification. It suggested that the findings by common

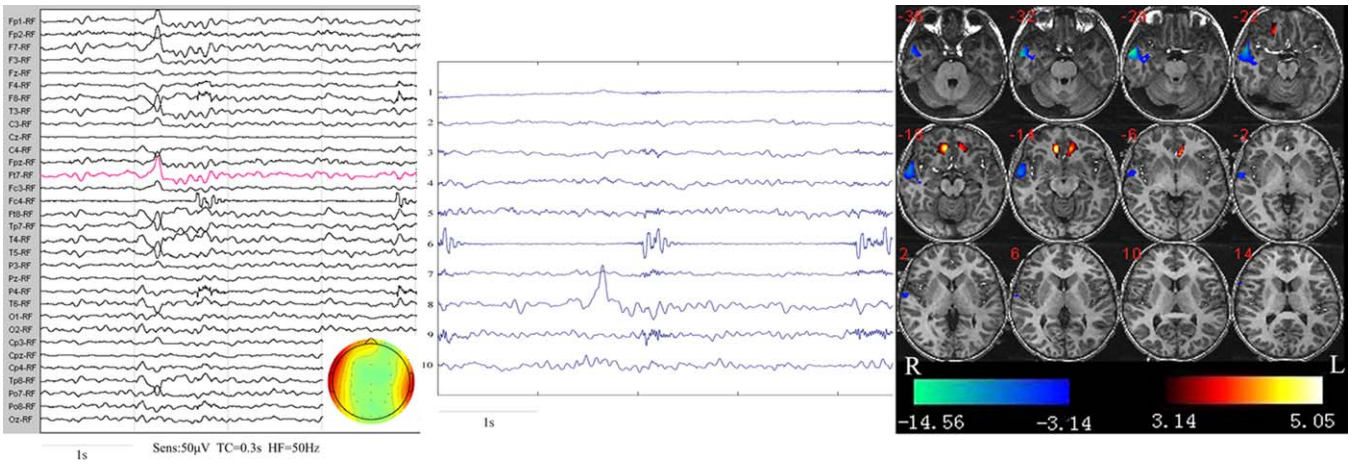

Figure 5 Type 2B IEDs in patient 2. Left: epileptic discharges recorded from the scalp in MR scanner in which the signal shown in red was classified by the expert. The epileptic activity was located at Ft7 T3 Fp1 F7 TP7. The topography of energy distribution during discharge was displayed. Middle: IC segments in the same time window as on the right. IC8 was selected to represent Type 2B. Right: fMRI results corresponding to IEDs on the left. Activation was observed in the bilateral frontal lobes, and deactivation was found in the left temporal lobes.

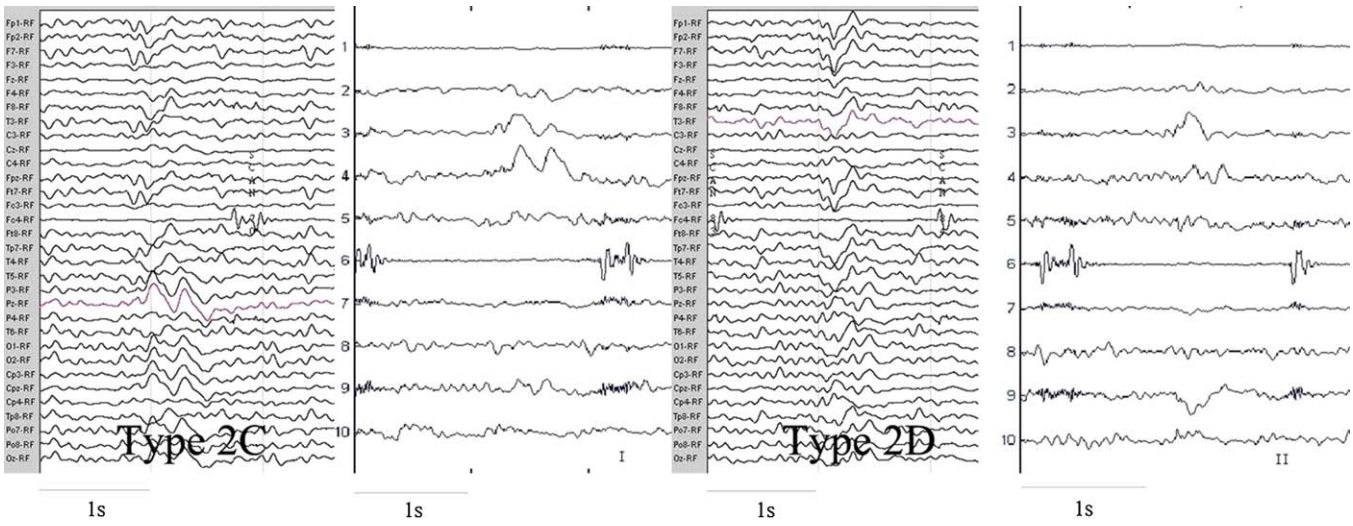

Figure 6 Type 2C and 2D IEDs in patient 2. These IEDs included 57.9% Type 2C and 15.8% Type 2D. Left: Scalp EEGs and corresponding ICs illustrating Type 2C IEDs. The slow wave activity was displayed at occipitoparietal regions. IC4 was selected to represent the Type 2C. Right: Scalp EEGs and corresponding ICs illustrating Type 2D IEDs. The high amplitude slow wave activity was mainly distributed at frontocentral regions. IC3 was selected to represent the Type 2D. No BOLD activity related to these IEDs was found.

method were consistent with that of our scheme (patients 4 and 6, for example). However, no activity was found in some IED categories (3B, 4B, 5C, 6D, 10C), whose ratios all were small. Further details are shown in Table 2. We compared the results acquired before and after the classification. Firstly, the IED type, whose map was similar to the result created by the common method, with a maximum ratio in the whole IEDs (i.e. patients 3, 4, 6; Table 2). It meant that the result by common method might reflect the major IED type and ignore others. Secondly, some additional regions were extracted (i.e. patients 5—10; Table 2) by our scheme. The additions were usually from IED type with low ratios. For example, for patient 5, the additional activation related to Type 5B (28%) was found in the bilateral frontal and parietal lobe (Table 2). It was admissive that the active pattern might be the corresponding metabolic activities of the epileptic discharge at bilateral central regions. Besides, the additions might be appropriate for interpretation, e.g. for patient 9 with right hippocampus atrophy, additional activation at right hippocampus (Type 9A) was consistent with the lesion (Table 2). However, some regions found before classification might be lost afterwards, such as the activation of patient 4 at parietal lobe (Table 2).

Discussions

Our findings demonstrate that IED classification, conducted by a combination of an ICA and a temporal correlation analysis between independent components and the raw EEG segment, is valuable. For patients whose activity cannot be identified by the common method, some foci that are consistent with electroclinical data could be localized using the classified IEDs as the GLM event related input. For the other patients with positive result acquired by the common method, similar active regions or additional regions can be imaged. Thus, our procedure partially solves the foci localization problem for patients with complex epileptic discharges.

Epileptic discharge classifications

In practice, when a clinically experienced neurophysiologist reviews the EEG of a patient, the scalp distribution, shape and frequency of IEDs are paid more attention to. In clinic practice, a preliminary classification based on the scalp distributions and shapes of IEDs can be acquired, but it strongly depends on the experience. Besides, the accuracy of the classification is affected by various artifacts in the EEG data. Epileptic discharges symmetrically displayed in all channels are distinctly different from the focal epileptic discharges in the number of the brain areas involved, thus we note it as a specific type which can be identified visually. However, the spatial distributions of various focal IEDs may partially overlap. For example, the 2 IED types in patient 1 had been classified as one type in the primary visual check, and GLM did not reveal the canonical HRF localizable foci before the classification.

ICA was first applied to EEG by Makeig (Makeig et al., 1996) and has been widely used since then. ICA algorithms can isolate artifact and neural activities from the EEG recordings (Makeig et al., 1999) and extract epileptic discharges from background EEG (Kobayashi et al., 1999), and separate spikes of different origins (Urrestarazu et al., 2006). EEG data acquired from the scalp in MR scanner contains significant artifacts, and the most prominent artifacts are from radio frequency magnetic change and ballistocardiography (BCG) (Gotman et al., 2006; Laufs et al., 2008). In the present study, the main artifacts were filtered out online by BE-MRI Toolbox, and the resulted EEG data was decomposed by ICA. The ICs related to the remaining artifacts and various epileptic discharges were identified, for example, the IC6 associated to artifact in patient 2 (Figs. 4—6). The general result was consistent with the previous studies

(Kobayashi et al., 2001; Srivastava et al., 2005; Jann et al., 2008).

Based on the principle of ICA, ICs representing IEDs are statistically independent. However, 1 IED may be decomposed or represented by a few ICs (Jann et al., 2008), this fact may raise problem in identifying an IC to represent an IED. Fortunately, what we really concerned about is to find an IC where the IED event is maximally reserved. In another word, our aim is not to look for an IC and use its waveform to replace the original IED waveform, so we assume that the independent component that maximally correlates with the selected raw EEG channel signal is the representation of the IED, and the epileptic activity events in this IC are considered as the events of this IED type. In this way, the classification can be done more easily and robustly. The results of patients 1 and 2 showed that our ICA classification was helpful in localizing the canonical HRF localizable foci.

Factors affecting sensitivity of imaging

Hemodynamic responses of IEDs in epileptic patients with different seizure types and in different age groups or even in different sessions in the same patient may show variability (Aguirre et al., 1998; Handwerker et al., 2004; Menz et al., 2006). In theory, a mismatched HRF as the regressor function is usually invalid to find the veritable activity. However, the actual hemodynamic response of an IED cannot be easily identified in a real dataset. In clinic practice, various epileptic discharges may be found in a patient with focal epilepsy, and the underlying source localization or presumed propagated zones should be different in general. For actual complex discharges consisting of various IEDs, different hemodynamic responses may be involved. It may fail to find any activities, even part of activities follows the canonical HRF. Our findings in Table 2 showed that no activity was found in some IED categories even positive result can be carried out by common method in these patients. It implicates that hemodynamic response related to these IED categories may be disaccord with canonical HRF which can be used to local for other IEDs or the whole IEDs. In this work, we are not searching for specific HRFs for different IED types, but to localize the localizable foci using the canonical HRF in SPM as the canonical HRF has been widely used in most EEG—fMRI studies (Jacobs et al., 2007; Gotman et al., 2006; Laufs et al., 2008).

For patients with complex epileptic discharge, the event ratio of each category may affect the imaging result. No significant BOLD change was observed, it may be because the event ratio of the localizable type was too small. The factor reduces the efficiency of the common GLM framework. On the contrary, if the active regions can be imaged for the largest ratio IEDs category, the positive result is acquired by the common method although no activity for some small ratio IEDs is found, such as patients 3—6, 10. Besides, the BOLD amplitude change also may distort the result. For patient 2, although there was only 1 IED (Type 2B), the active regions were localized because the signal was distinct. In fact, in Fig. 5, the average peak amplitude was 4.478% (range: 3.02—5.935) for the activated voxels and −8.024% (range: −8.93 to −7.118) for the deactivated voxels, while the usual value of the BOLD amplitude is less than 2% (Gu et al., 2001).

In summary, either the HRF, or the amplitude, or the event ratio may affect the detectability of an IED type. We pay special attention to those foci with the canonical HRF, which we call the localizable foci by the common GLM with canonical HRF, and we find the effect of the event ratio and the amplitude can be solved by an ICA based classification because both the two factors affect the signal (the localizable events) to noise (the un-localizable events and others) ratio, and the classification is actually a method to solve this problem, so we believe the IED classification is a crucial step in imaging the localizable BOLD activity.

Efficiency of the proposed scheme applied to clinic

By our scheme, some significant foci are extracted from the two patients whose foci cannot be identified by the usual GLM. For patient 1 with gray matter heterotopia, 1 IED type was localized with activation at the periheterotopia and deactivation in the lesioned and remote areas. This finding may suggest that the epileptic activities occurred in the lesioned and perilesion areas. In previous EEG—fMRI studies of epileptic patients with malformations of cortical development, the lesion, the surrounding cortex and distant area were found being involved in the interictal epileptic activities (Kobayashi et al., 2006; Tyvaert et al., 2008). Our findings are consistent with these previous studies. For patient 2, activations associated with the generalized discharges (Type 2A) were mainly localized at bilateral frontal and parietal cortex and thalamus, and no deactivation was found. Furthermore, the activations at the frontal lobes were more predominate. Such generalized discharges for patients with complex partial seizures may result from activity conduction between cortices via arciform fibers and the corpus callosum (Musgrave and Gloor, 1980), thus symmetrical activities are possible. Moreover, the thalamic response in this result is consistent with the previous study (Aghakhani et al., 2006). In other studies on idiopathic generalized epilepsy, activation at thalamus and deactivation at cortex were found, and the reason was supposed to be the activation of the thalamocortical network (Moeller et al., 2008; Gotman et al., 2005). For Type 2B, significant activities were found in the bilateral frontal lobes (positive) and left temporal lobe (negative). The epileptic activities in scalp EEG located at Ft7, T3, Fp1, F7, TP7. Activities at these electrodes of the frontotemporal region were concordant with active map resulted from fMRI imaging (Fig. 5). Although no direct evidence (such as local lesions) supports that the patient is a temporal lobe or frontal lobe epilepsy, we presume that the local activities resulted from Type 2B may indicate the irritative zone, and the widespread activities resulted from Type 2A may reflect the second spread network. For Type 2C and 2D, no activation was found, and the reason may be the mismatch HRF or others.

Applied to other eight patients with some active regions could be identified from the fMRI data by the common method, the activities can be obtained from at least one type of IED in the new method. In general, the map resulted from an IEDs category with maximum ratio is similar to that resulted without classification. It suggests that the findings

by common method may reflect the major IED type and ignore the others, and main activities are retained using our scheme. Comparing the results before and after the classification, some additional regions were extracted by our scheme. The additional activities were obtained from IED category with low ratio, which might be ignored in common method; or the addition was usually nearby or located at the lesion (patient 9, Table 2). It may be crucial to have some additional regions as epileptogenic zones, possibly indicating effects of different IED propagation (Laufs et al., 2007; Gotman et al., 2005). Furthermore, the additional regions may be considered as nodes to investigate the epileptogenic network and propagated network. Thus, the epileptic mechanism explanation is inappropriate when neglecting these components in the common method. However, it is possible that some regions found before classification could be lost after classification. The absence may be caused by the unstable epileptic discharge pattern of the corresponding region. During the ICA processing, the discharges in different time points (from the same spatial position) may be separated into different IC where they may mixed with other events and are of too small ratio to be imaged. The imaging for the unstable discharge should be investigated in future studies. Of course, the situation with varying patterns is unusual as the anatomo-functional abnormality of each region should have evolved to a stable state after long chronic discharges and seizure. In practice, we can combine the results received before and after the classification, the electroclinical feature and so on to interpret the epileptic mechanism in these patients.

Notes for the future

As shown above, for real data, some part of the neural activities from BOLD fMRI cannot be uncovered even with our scheme. To further improve the localization of various complex discharges, greater efforts are needed. To begin with, higher density EEG recordings may be applied in EEG—fMRI investigation, and the classification may be improved. Secondly, with better EEG recordings, an EEG inverse program may be conducted to de-blur the smearing effect of the head volume conductor (Yao et al., 2004), and then some more details of IEDs may be found and used in fMRI. Furthermore, the EEG and fMRI may be combined with a unified inverse framework for realizing high spatial and temporal resolution imaging of the underneath sources (Babiloni et al., 2005; He and Liu, 2008), and the specified functional networks of IEDs may be explored from the EEG—fMRI dataset too.

Conclusions

In this study, we aim to detect BOLD changes associated with complex epileptic discharges using the GLM-based SPM imaging. Based on our results, we conclude that the proposed scheme is effective for the analysis of EEG—fMRI data in which no BOLD change was found by common method in patients with complex epileptic discharges. In addition, even for cases in which foci can be identified by the general GLM, the scheme is still helpful in providing more detailed information of the foci.

Disclosure

The study was performed according to the standards set by the Declaration of Helsinki. The study was approved by the Ethics Committee of West China Hospital.

Conflicts of interest statement

None of the authors has any conflict of interest to disclose.

Acknowledgments

This project was funded by grants from the National Nature Science Foundation of China (30870655; 60736029; 30625024 and 30570474), the 973 Project (2007CB311001 and 2007CB512305), the 863 Program (2009AA02Z301 and 2008AA02Z408). This study was also sponsored by the program of International Cooperation and Exchange of National Natural Science Foundation of China (No. 30811120424).

References

Aghakhani, Y., Kobayashi, E., Bagshaw, A.P., Hawco, C., Benar, C.G., Dubeau, F., Gotman, J., 2006. Cortical and thalamic fMRI responses in partial epilepsy with focal and bilateral synchronous spikes. Clin. Neurophysiol. 117, 177—191.

Aguirre, G.K., Zarahn, E.D., Esposito, M., 1998. The variability of human, BOLD hemodynamic responses. NeuroImage 8, 360—369.

Babiloni, F., Cincotti, F., Babiloni, C., Carducci, F., Mattia, D., Astolfi, L., Basilisco, A., Rossini, P.M., Ding, L., Ni, Y., Cheng, J., Christine, K., Sweeney, J., He, B., 2005. Estimation of the cortical functional connectivity with the multimodal integration of high-resolution EEG and fMRI data by directed transfer function. NeuroImage 24, 118—131.

Bénar, C.G., Gross, D.W., Wang, Y., Petre, V., Pike, B., Dubeau, F., Gotman, J., 2002. The BOLD response to interictal epileptiform discharges. Neuroimage 17, 1182—1192.

Genovese, Christopher R., Lazar, Nicole A., Nichols, Thomas E., 2002. Thresholding of statistical maps in functional neuroimaging using the false discovery rate. NeuroImage 15, 870—878.

Comon, P., 1994. Independent component analysis, a new concept? J. Signal processing 36, 287—314.

Engel Jr., J., 2001. A proposed diagnostic scheme for people with epileptic seizures and with epilepsy: report of the ILAE Task Force on Classification and Terminology. Epilepsia 42, 796—803.

Friston, K.J., Holmes, A.P., Poline, J.B., Grasby, P.J., Williams, S.C.R., Frackowiak, R.S.J., Turner, R., 1995. Analysis of fMRI time-series revisited. NeuroImage 2, 45—53.

Friston, K.J., Josephs, O., Zarahn, E., Holmes, A.P., Rouquette, S., Poline, J., 2000. To smooth or not to smooth? Bias and efficiency in fMRI timeseries analysis. NeuroImage 12, 196—208.

Garreffa, G., Carnì, M., Gualniera, G., Ricci, G.B., Bozzao, L., De Carli, D., Morasso, P., Pantano, P., Colonnese, C., Roma, V., Maraviglia, B., 2003. Real-time MR artifacts filtering during continuous EEG/fMRI acquisition. Magn. Reson. Imaging 21, 1175—1189.

Gotman, J., Grova, C., Bagshaw, A., Kobayashi, E., Aghakhani, Y., Dubeau, F., 2005. Generalized epileptic discharges show thalamocortical activation and suspension of the default state of the brain. PNAS 102, 15236—15240.

Gotman, J., Kobayashi, E., Bagshaw, A.P., Beĭnar, C.G., Dubeau, F., 2006. Combining EEG and fMRI: a multimodal tool for epilepsy research. J. Magn. Reson. Imaging 23, 906—920.

Gu, H., Engelien, W., Feng, H., Silbersweig, D., Stern, E., Yang, Y., 2001. Mapping transient, randomly occurring neuropsychological events using independent component analysis. NeuroImage 14, 1432—1443.

Handwerker, D.A., Ollinger, J.M., D'Esposito, M., 2004. Variation of BOLD hemodynamic responses across subjects and brain regions and their effects on statistical analyses. NeuroImage 21, 1639—1651.

He, B., Liu, Z., 2008. Multimodal functional neuroimaging integrating functional MRI and EEG/MEG. IEEE Rev. Biomed. Eng. 1, 23—40.

Hyvärinen, A., 1999. Fast and robust fixed-point algorithms for independent component analysis. IEEE Trans. Neural Netw. 10, 626—634.

Ives, J.R., Warach, S., Schmitt, F., Edelman, R.R., Schomer, D.L., 1993. Monitoring the patient's EEG during echo planar MRI. Electroencephalogr. Clin. Neurophysiol. 87, 417—420.

Jacobs, J., Kobayashi, E., Boor, R., Muhle, H., Stephan, W., Hawco, C., Dubeau, F., Jansen, O., Stephani, U., Gotman, J., Siniatchkin, M., 2007. Hemodynamic responses to interictal epileptic discharges in children with symptomatic epilepsy. Epilepsia 48, 2068—2078.

Jann, K., Wiest, R., Hauf, M., Meyer, K., Boesch, C., Mathis, J., Schroth, G., Dierks, T., Koenig, T., 2008. BOLD correlates of continuously fluctuating epileptic activity isolated by independent component analysis. NeuroImage 42, 635—648.

Kobayashi, E., Bagshaw, A.P., Grova, C., Gotman, J., Dubeau, F., 2006. Grey matter heterotopia: what EEG—fMRI can tell us about epileptogenicity of neuronal migration disorders. Brain 129, 366—374.

Kobayashi, K., James, C.J., Nakahori, T., Akiyama, T., Gotman, J., 1999. Isolation of epileptiform discharges from unaveraged EEG by independent component analysis. Clin. Neurophysiol. 110, 1755—1763.

Kobayashi, K., Merlet, I., Gotman, J., 2001. Separation of spikes from background by independent component analysis with dipole modeling and comparison to intracranial recording. Clin. Neurophysiol. 112, 405—413.

Laufs, H., Hamandi, K., Salek-Haddadi, A., Kleinschmidt, A.K., John, S., Lemieux, L., 2007. Temporal lobe interictal epileptic discharges affect cerebral activity in ''Default Mode'' brain regions. Hum. Brain Mapp. 28, 1023—1032.

Laufs, H., Daunizeau, J., Carmichael, D.W., Kleinschmidt, A., 2008. Recent advances in recording electrophysiological data simultaneously with magnetic resonance imaging. NeuroImage 40, 515—528.

Lemieux, L., Laufs, H., Carmichael, D.W., Paul, J.S., Walker, M.C., Duncan, J.S., 2008. Noncanonical spike-related BOLD responses in focal epilepsy. Hum. Brain Mapp. 29, 329—345.

Li, Q., Luo, C., Yang, T., Yao, Z., He, L., Liu, L., Xu, H., Gong, Q., Yao, D., Zhou, D., 2009. EEG—fMRI study on the interictal and ictal generalized spike-wave discharges for patient with childhood absence epilepsy. Epilepsy Res. 87, 160—168.

Liston, A.D., De Munck, J.C., Hamandi, K., Laufs, H., Ossenblok, P., Duncan, J.S., Lemieux, L., 2006. Analysis of EEG—fMRI data in focal epilepsy based on automated spike classification and Signal Space Projection. NeuroImage 31, 1015—1024.

Lu, Y., Bagshaw, A.P., Grova, C., Kobayashi, E., Dubeau, F., Gotman, J., 2006. Using voxel-specific hemodynamic response function in EEG—fMRI data analysis. NeuroImage 32, 238—247.

Luo, C., Li, Q., Lai, Y., Xia, Y., Qin, Y., Liao, W., Li, S., Zhou, D., Yao, D., Gong, Q., in press. Altered functional connectivity in default mode network in absence epilepsy interictal duration without IED: a resting-state fMRI study. Hum. Brain Mapp., doi:10.1002/hbm.21034.

Makeig, S., Bell, A.J., Jung, T.P., Sejnowski, T.J., 1996. Independent component analysis of electroencephalographic data. Adv. Neural Inf. Process. Syst. 8, 145—151.

Makeig, S., Westerfield, M., Jung, T.P., Covington, J., Twonsend, J., Sejnowski, T.J., Courchesne, E., 1999. Functionally independent components of the late positive event-related potential during visual spatial attention. J. Neurosci. 19, 2665—2680.

Menz, M.M., Neumanna, J., Müllera, J., Zysse, S., 2006. Variability of the BOLD response over time: an examination of within-session differences. NeuroImage 32, 1185—1194.

Moeller, F., Siebner, H.R., Wolff, S., Muhle, H., Boor, R., Granert, O., Jansen, O., Stephani, U., Siniatchkin, M., 2008. Change in activity of striato—thalamo—cortical network precede generalized spike wave discharges. NeuroImage 39, 1839—1849.

Musgrave, J., Gloor, P., 1980. The role of the corpus callosum in bilateral interhemispheric synchrony of spike and wave discharge in feline generalized penicillin epilepsy. Epilepsia 21, 369—378.

Rodionov, R., De Martino, F., Laufs, H., Carmichael, D.W., Formisano, E., Walker, M., John, S., Duncan, Lemieux, L., 2007. Independent component analysis of interictal fMRI in focal epilepsy: comparison with general linear model-based EEG-correlated fMRI. NeuroImage 38, 488—500.

Salek-Haddadi, A., Diehl, B., Hamandi, K., Merschhemke, M., Liston, A., Friston, K., Duncan, J.S., Fish, D.R., Lemieux, L., 2006. Hemodynamic correlates of epileptiform discharges: an EEG—fMRI study of 63 patients with focal epilepsy. Brain Res. 1088, 148—166.

Srivastava, G., Crottaz-Herbette, A., Lau, K.M., Glover, G.H., Menon, V., 2005. ICA-based procedures for removing ballistocardiogram artifacts from EEG data acquired in the MRI scanner. NeuroImage 24, 50—60.

Tyvaert, L., Hawco, C., Kobayashi, E., LeVan, P., Dubeau, F., Gotman, J., 2008. Different structures involved during ictal and interictal epileptic activity in malformations of cortical development: an EEG—fMRI study. Brain 131, 2042—2060.

Urrestarazu, E., Iriarte, J., Artieda, J., Alegre, M., Valencia, M., Viteri, C., 2006. Independent component analysis separates spikes of different origin in the EEG. J. Clin. Neurophysiol. 23, 72—78.

Yao, D., Yin, Z., Tang, X., Arendt-Nielsen, L., Chen, C.A.N., 2004. High-resolution electroencephalogram (EEG) mapping: scalp charge layer. Phys. Med. Biol. 49, 5073—5086.